Alexandria Engineering Journal (2023) 66, 845–859

HOSTED BY

ELSEVIER

Alexandria University

Alexandria Engineering Journal

www.elsevier.com/locate/aej
www.sciencedirect.com

Threading holder based on axial metal cylinder pins to reduce tap risk during reversion instant

P. Fernández-Lucio [a,b], A. Gil Del Val [c,d], S. Plaza [a,b], O. Pereira [a,*], A. Fernández-Valdivielso [a], L.N. López de Lacalle [a,b]

[a] *CFAA- Aeronautics Advanced Manufacturing Center, University of the Basque Country (UPV/EHU), Biscay Science and Technology Park, Ed. 202, Zamudio, Spain*
[b] *Department of Mechanical Engineering, University of the Basque Country (UPV/EHU), Plaza Torres de Quevedo s/n, 48013 Bilbao, Spain*
[c] *Tecnalia Research & Innovation. Parque Científico y Tecnológico de Gipuzkoa, Mikeletegi Pasealekua, 7, 20009 Donostia, Spain*
[d] *Universidad Internacional de La Rioja (UNIR), Av. de la Paz, 137, 26006 Logroño, Spain*

Received 6 June 2022; revised 20 September 2022; accepted 23 October 2022
Available online 05 November 2022

KEYWORDS

Tapping;
Toolholder;
Difficult-to-cut tapping;
Tapping reversion instant

Abstract Internal thread profiles are used widely in manufacturing processes with the aim of assembling/disassembling different components during maintenance activities from the aeronautics sector until common industrial parts. The threading process is one of the last operations carried out to obtain those components, and consequently, it is an operation of high added value. Threading is a complex operation that must carefully synchronize the rotation with the feed movements to avoid tool breakage during the instant of tapping reversion stage. In order to avoid this risk, several toolholders were developed present in the literature but deficiencies in terms of stability and productivity. Therefore, in this work, a new toolholder is proposed in which the common springs used to mitigate the lack of perfect synchronization between rotation and feed movements are replaced by elastic metal pins achieving a torsional compliance toolholder. The results show that the use of the proposed toolholder implies not only a productivity increase but also a surface integrity improvement as well as a stress reduction that the cutting tap is subjected and thus, achieving a substantial improvement in the current tapping processes. In particular, the use of the proposed toolholder implied a 75% reduction of the maximum stress achieved in the reversal instant, improving 20% tool life with an increase of 30% cutting speed. Therefore, the use of the proposed toolholder implies a substantial improvement in the current tapping processes.

* Corresponding author at: University of the Basque Country (UPV/EHU), CFAA- Aeronautics Advanced Manufacturing Center, University of the Basque Country (UPV/EHU), Biscay Science and Technology Park, Ed. 202, Zamudio, Spain.
E-mail address: octaviomanuel.pereira@ehu.eus (O. Pereira).

Peer review under responsibility of Faculty of Engineering, Alexandria University.

https://doi.org/10.1016/j.aej.2022.10.060
1110-0168

1. Introduction

Internal thread profiles are commonly used in industrial manufacturing assemblies but also in home appliances and medical mechanisms because a good quality profile allows to assemble/disassemble machine/device components for maintenance. However, this manufacturing process, known as tapping or threading, implies a high-quality level. Besides, this operation, called tapping, is the last one in a manufacturing cell when the industrial part just has accumulated all the added value [1–2], so a bad hole is a waste of time and money.

Tapping is a manufacturing process to produce a fine thread inside a drilled hole into the workpiece material. There are two main processes for internal thread manufacturing: forming (form or roll taps are called the tools) and machining (cutting taps). The former generates threads by plastic deformation, whereas the latter cutting tap removes material sculpting the thread profile. Focusing on the last one, thread quality depends on the quality of the previous drilled hole (initial diameter), but it also depends on the number of active teeth when tapping a thread [3] because the more, the better, and the synchronism between machine rotational and feed movements [4–5]. These three characteristics define the high complexity of this manufacturing operation.

It should be noted tapping operations represent 30 % of total manufacturing time in some applications [6], and so manufacturing companies demand an operation time reduction in order to improve productivity and competitivity.

The need for precise synchronism between rotational and axial tool movements is key to avoid uncontrolled tapping tool breakage. Good threading implies preventing additional reparation on the workpiece and consequently loss of time and increases in costs.

Special toolholders are used for tapping operations with the aim of offsetting the lack of perfect synchronization of rotation and feed movements. One toolholder type, known as the "axial compliance toolholder", is characterized by owning an internal mechanism based on an internal spring, which is used as a clutch for absorbing these synchronization errors and the gaps between feed and rotational speed when the direction of the rotation is reversed. Any tap must get back using the reverse just produced thread in the previous movement. The most reliable system is a toolholder equipped with a clutch based on planetary gears, which inverse the movement itself (Tapmatic® is the well-known brand), but it implies a large diameter toolholder to use in universal machining centers; complex to manage in the tool magazine. The system is used in automatic threading machines, always doing the same operation.

In the literature, many researches were carried out over the last decade using this kind of toolholders, trying to improve the tapping process through optimizing tool geometry, cutting conditions, developing predictive models, using new coatings and improving lubricooling techniques, among others. In particular, Uzun et al. [7] described the influence of cryogenic treatment on cut and form taps. Gil Del Val et al. [8] studied the wear mechanisms when tapping nodular cast iron at high-speed conditions. Pereira et al. [9] statistically analyzed the influence of some factors (cutting speed and the method of application of cutting fluid) when threading three different grey cast irons. In the following publication, they studied the process behavior of secondary features (thread length, coating, feed rate and hole diameter) and proposed a torque and force distribution with a new floating system based on an adaptive table to compensate for small synchronism errors between rotation and feed [10]. A similar analysis was carried out by Oliveira et al. [11], where the use of an adaptive table during threading operations was compared with the use of axial compliance toolholders. In this case, similar results were obtained with both systems, respectively. Elosegui et al. [12] analyzed the cutting performance and selected the best physical vapor deposition (PVD) coating when tapping austempered ductile iron 900. Related to thread quality and tapping fault, Zawada-Tomkiewicz et al. [13] studied the quality of the metric screw thread based on the closed-loop manufacturing (CLM) system. Freitas et al. [14] proposed a quality method to compare the thread profile and the ISO metric thread basic profile according to iSO-68–1 and ISO 68–2 when tapping carbon fiber reinforced polymer (CFRP) samples. Monka et al. [2] studied the tap failure when machining C45. Focusing on new lubricant and tap geometry, Ni et al. [15] proposed a metalworking lubrication of vegetable oil. They analyzed the effect of graphene additive on the torque when tapping ADC12 aluminum alloy. A coated tap with the maximum helix angle and without chip breaker was selected in threaded blind holes. Agapiou et al. [4] and Ahn et al. [5] also analyzed the threading performance at high speed cutting conditions. Lorentz [16] optimized the tap geometry using principal component analysis (PCA). Three other authors developed classification strategies for three common faults (tap wear level, misalignment between hole and tap axis and under/oversized predrilled holes diameter) based on condition probability functions, neuronal networks, PCA and neuronal networks, respectively [17–19]. Related to modeling, Mezentsev et al. [20] developed a predictive model to assure thread quality in tapping operations. Finally, Gil Del Val et al. [21] proposed a monitoring system based on PCA and statical control of the process to guarantee thread quality during a tapping operation.

Currently, Pereira et al. [22] studied the torque and temperature behaviors for each individual thread to improve the new tap geometries, Polvorosa et al. [23] proposed a cutting-edge control based on cutting forces and torque during tapping operation in Inconel 718 specimens and Gil Del Val et al. [24] studied the wear evolution of conical and cylindrical teeth when tapping nodular cast iron at high-speed conditions.

Nevertheless, the topic of synchronizing movements of tapping processes through improving conventional toolholders was not deeply dealt. In this line, there are three researches found. The first one, carried out by Pereira et al. [10], avoided the synchronicity errors using their own developed floating system. In the second one, Dos Santos et al. [25] selected the best tap geometry when machining workpieces of SAE 1020 steel using a commercial semi-rigid axial compensation mechanism based on balls and elastomers to reduce these kind of errors. In the last one, Wan et al. [26] developed a predicting feed error-induced force model using a toolholder with compensation function to avoid this fault in the tapping process.

Therefore, the novelty of the work here presented stems from the idea of improving tapping processes through the use of a torsional compliance toolholder in which the spring is replaced by elastic metal pins, which allows eliminating shocks during the tapping reversion movement without affecting thread quality and at the same time providing better preci-

Table 1 The four types of toolholders.

	Automatic clutch toolholder	Axial compliance toolholder	Total rigid	New one, torsional compliance toolholder
Volume	+ + +	+ +	+	+
Possibility to be on machine magazine	Null	+ +	+ + +	+ + +
Reliability	+ + +	+ +	Depends on machine precision absolutely	+ +
Cost	+ + +	+ + +	+	+ +
Requirement of feed-rotation precision	+	+ +	+ + + +	+ +
Productivity	+ + + +	+ +		+ + +

Legend: + + + High, + + moderate, + low.

sion and higher stiffness, required in the current industry. Table 1 summarizes the technical characteristics of the three types of toolholders and the new one proposed.

For the validation of this new kind of toolholder, its behavior during the tapping reversion instant – which is the critical stage in threading operations – was compared with a conventional axial compliance toolholder by a Finite Element Method (FEM) simulation. After that, empirical tests were carried out in which the improvement effect on real threading operations through tool life and surface integrity of the threads performed was analyzed between both toolholders. The results show that by using the proposed toolholder, not only tapping tool life is increased but also thread surface integrity is improved.

2. Methodology

2.1. Toolholders description

Regarding the two toolholders tested, they differ mainly in the mode of operation in the reversion instant. The first one is a conventional axial compliance toolholder, which has a spring to absorb the backlash presented by the axial movement when the direction is changed during thread manufacturing in the reversal instant.

The other one is the toolholder proposed for improving the threading process. This toolholder is a torsional compliance one that has two elastic metal cylinder pins to absorb shocks and hits when the machine spindle/tool changes rotation avoiding problems associated with this threading stage. HSS cutting taps usually break at this moment, hence improving the importance of the toolholder at this stage. Fig. 1 schematizes the difference between the conventional axial compliance toolholder and the proposed one (torsional compliance toolholder).

For designing the size of the pins, a previous test was carried out in which spindle power consumption was measured with Vydas® UPC-E power cell with the aim of obtaining the cutting stress achieved during the reversion instant. In particular, ten threads were carried out with a cutting speed of 15 m/min and the results obtained are shown in Fig. 2.

The results show that the maximum peak is obtained in the reversion instant, being near 3.5 kW; therefore, this was the value established to determine the pin diameter in order to support the most extreme condition during the toolholder useful life. In particular, to calculate pins diameter, the force achieved on the cutting edge was first calculated due to the reversion movement. After, this value force was transmitted throw the moment to the pins. Finally, with the force obtained in the pins, Von Misses' theorem was applied to determine the pins diameter using a security factor of 1.5.

Therefore, first, equation (1) was applied to obtain the force achieved on the cutting edge during the reversion instant due to this equation relates spindle electrical power consumption with the cutting force obtained on the cutting edge [27].

$$P_c = P_{c0} + \frac{F_c v_c}{60} \rightarrow \boldsymbol{F_c} = \frac{(\boldsymbol{P_c} - \boldsymbol{P_{c0}}) \cdot 60}{\boldsymbol{v_c}} \quad (1)$$

In this equation, F_c is the force achieved during the reversion instant; P_c is the electric power consumed by the spindle (3.5 kW); P_{c0} is the idle power consumption of the spindle, which in this case was 0.35 kW; and finally, v_c is the cutting speed which was 15 m/min. Applying these values to equation (1), the force (F_c) achieved at this stage was 12.6 kN. Afterward, equation (4) is obtained by equaling equation (2) and equation (3) (through momentum transmitted, M_c), thus getting the force applied to each pin (F_{pin}).

$$M_c = F_c \cdot R_{tool} \quad (2)$$

$$M_c = 2F_{pin} \cdot R_{pin} \quad (3)$$

$$F_c \cdot R_{tool} = 2F_{pin} \cdot R_{pin} \rightarrow \boldsymbol{F_{pin}} = \frac{\boldsymbol{F_c} \cdot \boldsymbol{R_{tool}}}{2\boldsymbol{R_{pin}}} \quad (4)$$

In this case, the tool radius (R_{tool}) was 5 mm and the radius where pins were placed (R_{pin}) was 6.4 mm. Then, the force applied to each pin (F_{pin}) resulted in 4.922 kN.

Once the force applied in each pin was obtained, Von Misses' theorem was applied where direct stress is zero because pins are working under pure shear stress and therefore Von Misses stress resulting as is shown in equation (5).

$$\sigma_{VM} = \sqrt{\sigma^2 + 3\tau^2}; in this case \sigma = 0 \rightarrow \boldsymbol{\sigma_{VM}} = \sqrt{3}\boldsymbol{\tau} \quad (5)$$

On the other hand, the limit yield stress of the pins steel (σ_{lim}) was 448 N/mm^2 and the security factor (n) was established at 1.5 to calculate the admissible yield. This admissible yield (σ_{adm}) has to be greater or equal to Von Misses' stress in order to ensure the pins support working conditions, as shown in equation (6).

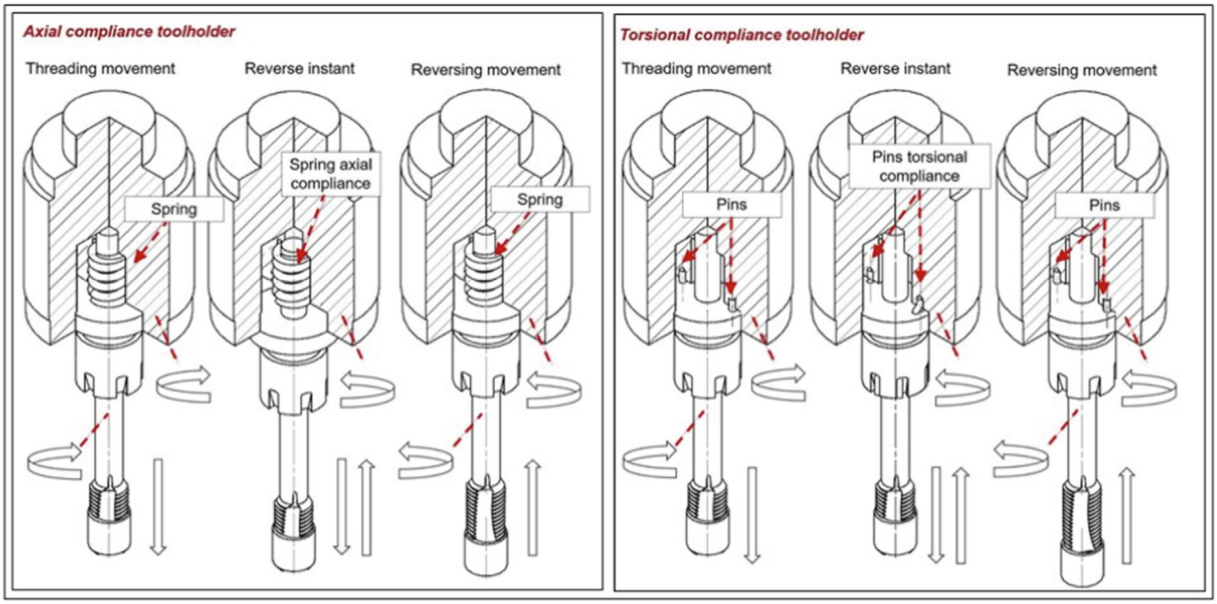

Fig. 1 Scheme of the axial and torsional compliance toolholders.

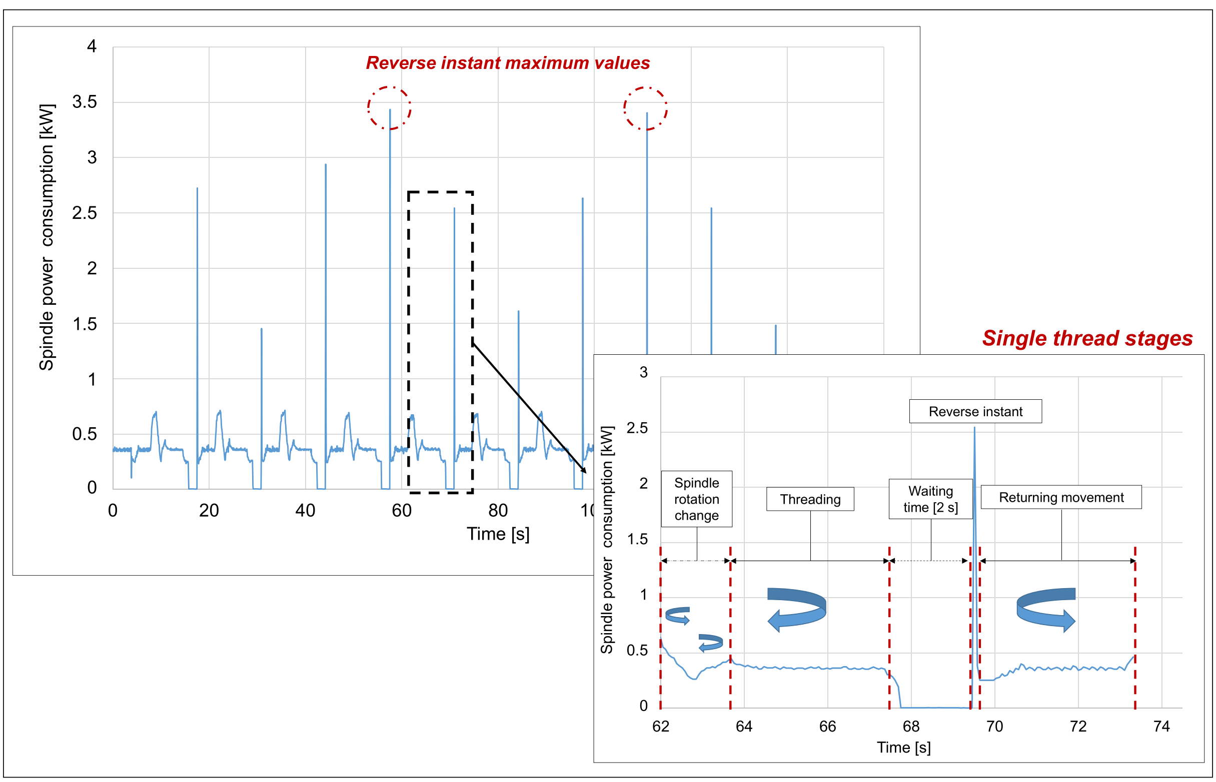

Fig. 2 Spindle power consumption obtained in the previous test and single thread stages.

$$\sigma_{VM} \leq \sigma_{adm} = \frac{\sigma_{lim}}{n} \quad (6)$$

Besides, the shear stress results from the quotient between the force applied on the pin and the pin section (equation (7)), which, combined with Von Misses' yield stress (equation (8)), implies the determination of the pin diameter needed to design the proposed toolholder (equation (9)).

$$\tau = \frac{F_{pin}}{\Omega}; where \Omega = \pi \frac{d^2}{4} \quad (7)$$

$$\sigma_{adm} = \frac{\sigma_{lim}}{n} \rightarrow \tau = \frac{\sigma_{lim}}{n\sqrt{3}} \quad (8)$$

$$\frac{F_{pin}}{\pi \frac{d^2}{4}} = \frac{\sigma_{lim}}{n\sqrt{3}} \rightarrow \boldsymbol{d} = \sqrt{\frac{4\sqrt{3}\boldsymbol{F_{pin}} \cdot \boldsymbol{n}}{\boldsymbol{\pi} \cdot \boldsymbol{\sigma_{lim}}}} \quad (9)$$

The resulting diameter, in this case was 6 mm, which was the value applied to each pin to manufacture the torsional compliance toolholder and compare its behavior with the axial compliance tool holder described above. Fig. 3 sums up graphically the process carried out to obtain the diameter of the pins.

2.2. FEM simulation setup

The simulations were carried out in Ansys® software through static structural modulus. In order to model the behavior of the toolholders at the tapping reversion instant stage, the CAD used was simplified into three parts: an external case, the elastic systems in each toolholder (axial spring and elastic metal pins, respectively), and the chuck which joins the case with the elastic system and the tool. Regarding the tool, it was modeled as a high-speed steel M10 cutting tap. Finally, the thread was modeled and positioned accordingly in the tap to simulate the tapping reversion instant once the thread was performed. Fig. 4 shows the simulation setup carried out.

The meshing process was applied to the parts defined as flexible, that is, the elastic system, the cutting tap and the thread. These parts are the ones that influence in the transference of the rotary motion from the spindle to the cutting edge. The kind of mesh used was based on quad and tri mesh elements with a smooth transition from the tool core to the cutting zone, where the element size target was 0.05 mm to optimize computational costs. Fig. 5 shows the mesh carried to both models.

Regarding connections between the CAD parts that form the FEM model, the tap is bonded to the chuck and the M10 thread is fixed to the ground. In the case of the axial compliance toolholder, the spring is bonded to the case and chuck,

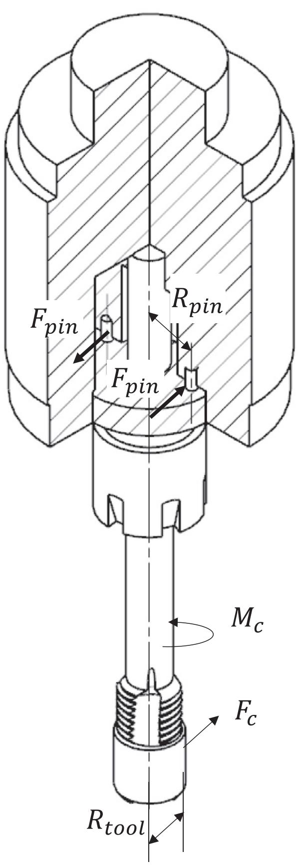

$$P_c = P_{c0} + \frac{F_c v_c}{60} \rightarrow \boldsymbol{F_c} = \frac{(\boldsymbol{P_c} - \boldsymbol{P_{c0}}) \cdot \mathbf{60}}{\boldsymbol{v_c}}$$

$$F_c = \frac{(3500 - 350) \cdot 60}{15} \rightarrow \boldsymbol{F_c} = \mathbf{12.6}\ \boldsymbol{kN}$$

$$M_c = F_c \cdot R_{tool} \qquad M_c = 2F_{pin} \cdot R_{pin}$$

$$F_c \cdot R_{tool} = 2F_{pin} \cdot R_{pin}$$

$$\boldsymbol{F_{pin}} = \frac{\boldsymbol{F_c} \cdot \boldsymbol{R_{tool}}}{\mathbf{2}\boldsymbol{R_{pin}}} \rightarrow F_{pin} = 4.922\ kN$$

Von Misses theorem

$$\sigma_{VM} = \sqrt{\sigma^2 + 3\tau^2}\ ;\ in\ this\ case\ \sigma = 0$$

$$\boldsymbol{\sigma_{VM}} = \sqrt{\mathbf{3}}\boldsymbol{\tau} \leq \boldsymbol{\sigma_{adm}}$$

$$\sigma_{adm} = \frac{\sigma_{lim}}{n} \rightarrow \tau = \frac{\sigma_{lim}}{n\sqrt{3}}$$

$$\boldsymbol{\tau} = \frac{\boldsymbol{F_{pin}}}{\boldsymbol{\Omega}};\ where\ \Omega = \pi\frac{d^2}{4} \rightarrow \frac{F_{pin}}{\pi\frac{d^2}{4}} = \frac{\sigma_{lim}}{n\sqrt{3}}$$

$$\boldsymbol{d} = \sqrt{\frac{\mathbf{4}\sqrt{\mathbf{3}}\boldsymbol{F_{pin}} \cdot \boldsymbol{n}}{\boldsymbol{\pi} \cdot \boldsymbol{\sigma_{lim}}}} \rightarrow d = 6\ mm$$

Fig. 3 Pins diameter determination to be applied in the torsional compliance toolholder.

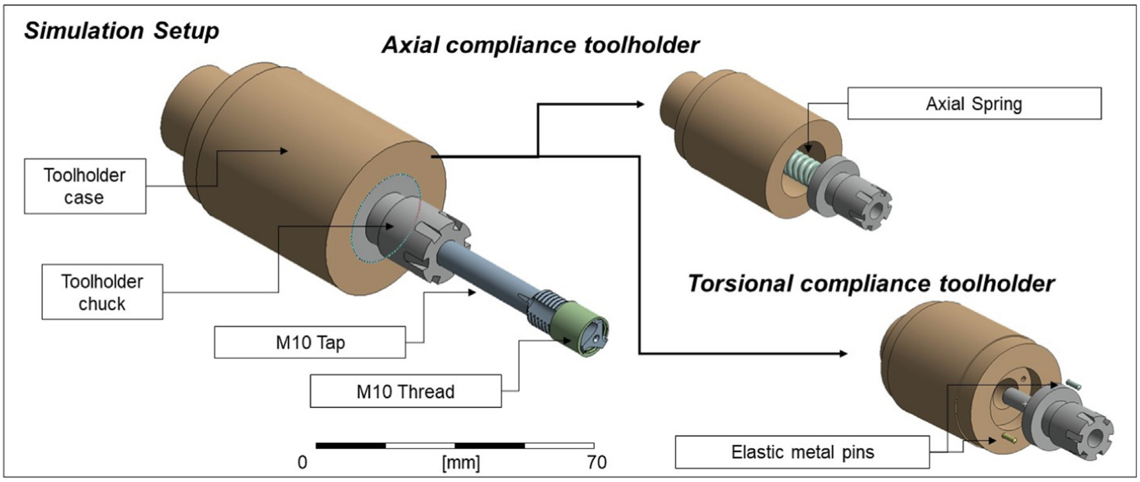

Fig. 4 CADs for modeling turn change once the thread is performed.

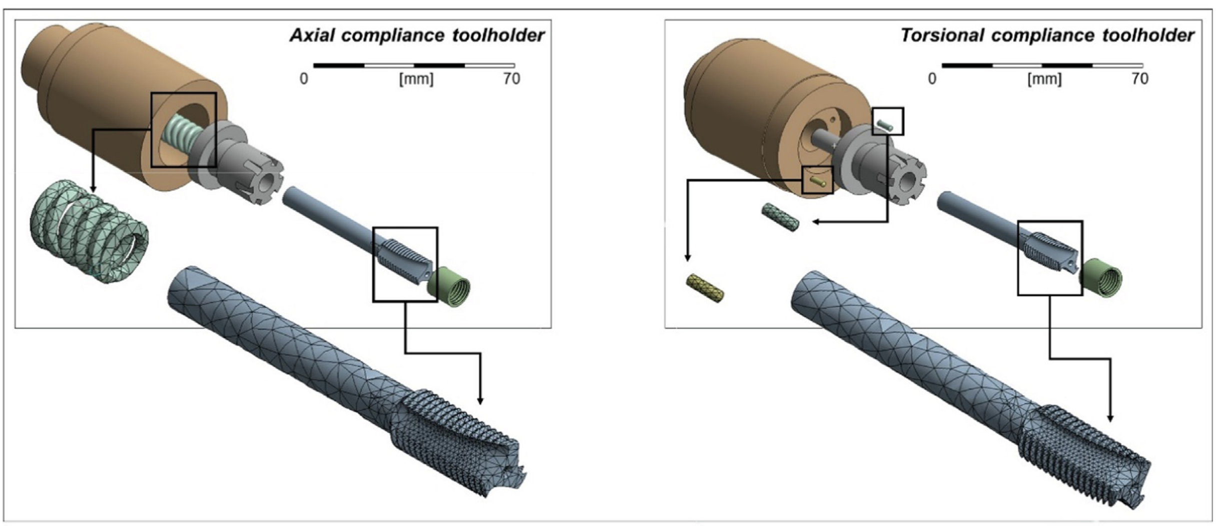

Fig. 5 Mesh carried out for both simulations.

respectively. In the case of the torsional compliance toolholder, the upper faces of the elastic metal pins are bonded to the case. The chuck and the case were connected in order to fix the axial movement, therefore allowing only the rotational movement. Fig. 6 sums up the connections established to carry out the simulation.

Concerning cutting conditions, the cutting speed and the axial feed of the tap in the model were defined by establishing a rotational speed and axial one, respectively. In particular, the values established in the FEM simulation were 15 m/min of cutting speed (8 rad/s) and 720 mm/min of feed (12 mm/s) as industrial representative values.

Finally, to introduce the tapping reversion instant effect in the simulation, the axial and rotational movements were desynchronized; that is, the axial movement starts in the initial stage and the rotational one 0.3 s later. This value was obtained through the measures carried out in a previous test in which ten threads were carried out. During the process, the spindle's power consumption and axial consumption with two Vydas® UPC-E power cells were measured. Once the values of the power consumptions were acquired, the delay between the axial and rotational movement was obtained. Therefore, the tapping reversion instant effect once the thread is finished could be performed.

2.3. Experimental setup

Regarding empirical tests, they were carried out in an Ibarmia® ZV25/U600 5-axis machining center with a maximum spindle power of 15 kW. The workpiece material used for toolholder testing was 42CrMo4 steel, which was previously face milled to obtain a perpendicular face to carry out the test campaign. This steel is characterized by presenting a high percentage of abrasive/hardening alloying elements. Its chemical composition and mechanical properties are shown in Table 2**.**

The threads carried out were on blind holes. Tapping tools were high steed speed (HSS) M10 cutting taps P2054905 from EMUGE-Franke®, coated with TiN. The previous drilling was done with a HSS drilling tool of 8.5 mm diameter just before each test to avoid alignment problems between the hole

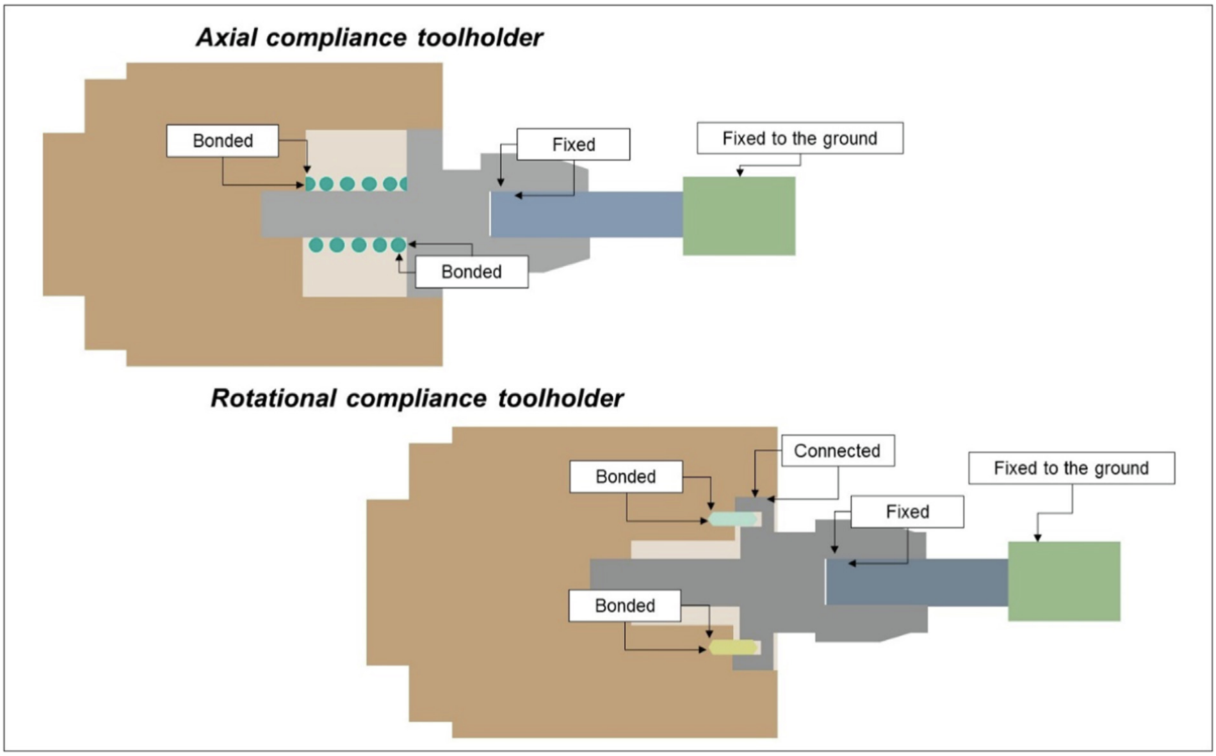

Fig. 6 FEM connections established.

Table 2 Chemical composition and Mechanical Properties.

Chemical Composition [%]									
C	Mn	Si	P	S	Cr	Mo	Ni	Cu	Al
0.39	0.83	0.27	0.007	0.029	1.05	0.226	0.015	0.007	0.022

Mechanical properties			
Rm [N/mm^2]	Re [N/mm^2]	A [%]	Hardness [HB]
791	628	19	240

and the tapping tool axis. The depth of each tap was 20 mm and the overhang of the cutting taps was 65 mm. Test sets carried out were two:

1. In the first stage, the conventional axial compliance toolholder and the new proposed torsional compliance toolholder behaviors were compared. In this case, cutting speed was based on industrial recommended values by the manufacturers for this kind of toolholder-tool, that is, 15 m/min.
2. A second stage with the proposed toolholder in which cutting speed was modified using the proposed toolholder until achieving a similar tool obtained in the previous battery with the conventional toolholder. In particular, cutting speed tests were 10 m/min, 15 m/min and 20 m/min.

During the tests, spindle power consumption was measured with a Vydas® UPC-E power cell installed in the machine, and several stops were carried out in order to measure tool edge wear in the incidence face. Each test was carried out three times and obtained the average values. Test stop criteria were based on ISO 3685 and a "go/no go" gauge. Once the battery tests were completed, taps surface integrity was analyzed with an infinite-focus Alicona® microscope to validate the use of the proposed toolholder. The experimental setup carried out is presented in Fig. 7.

3. Results and discussion

Fig. 8 shows the simulation results related to the equivalent stress caused in the cutting tap when the tapping reversion instant stage is achieved with both toolholders. In both cases, the maximum stress is obtained on the second cutting edge of the cutting tap. However, the values are different. In particular, when the axial compliance toolholder is used, the value obtained is 3,365 MPa and when the proposed one (torsional compliance toolholder) is used, the value is 870 MPa; thus, the use of the new toolholder implies a reduction of the maximum stress of ≈75 %. The next zone where this value increase

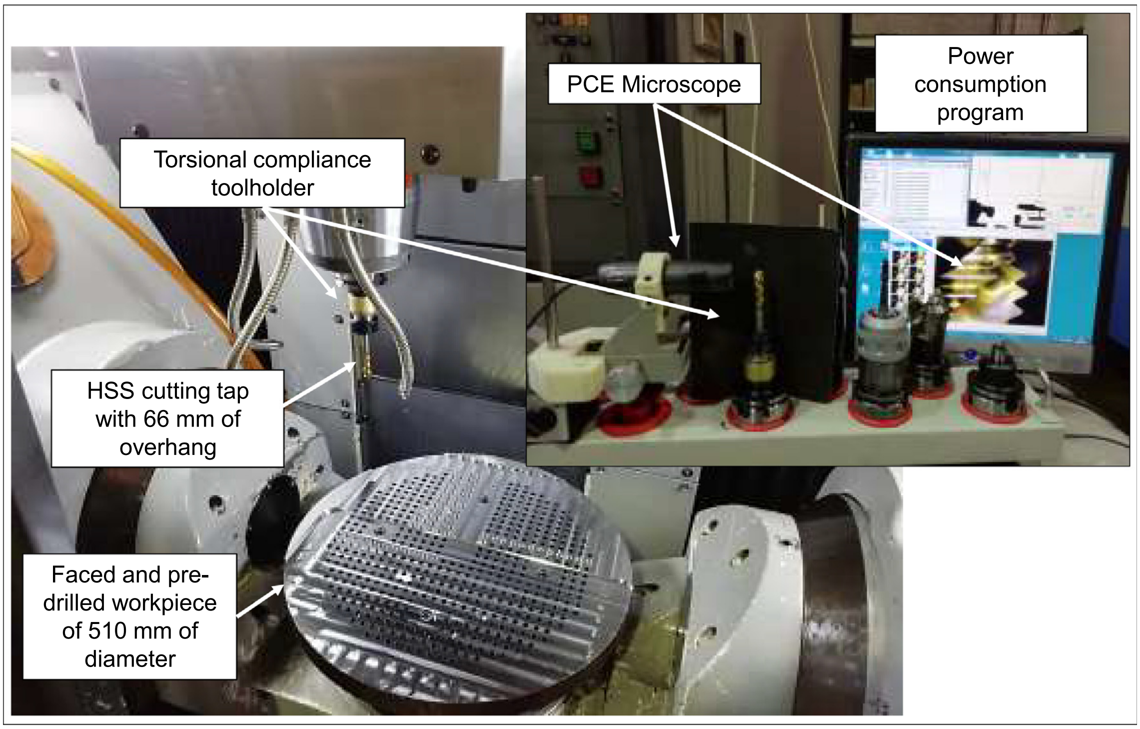

Fig. 7 Experimental setup.

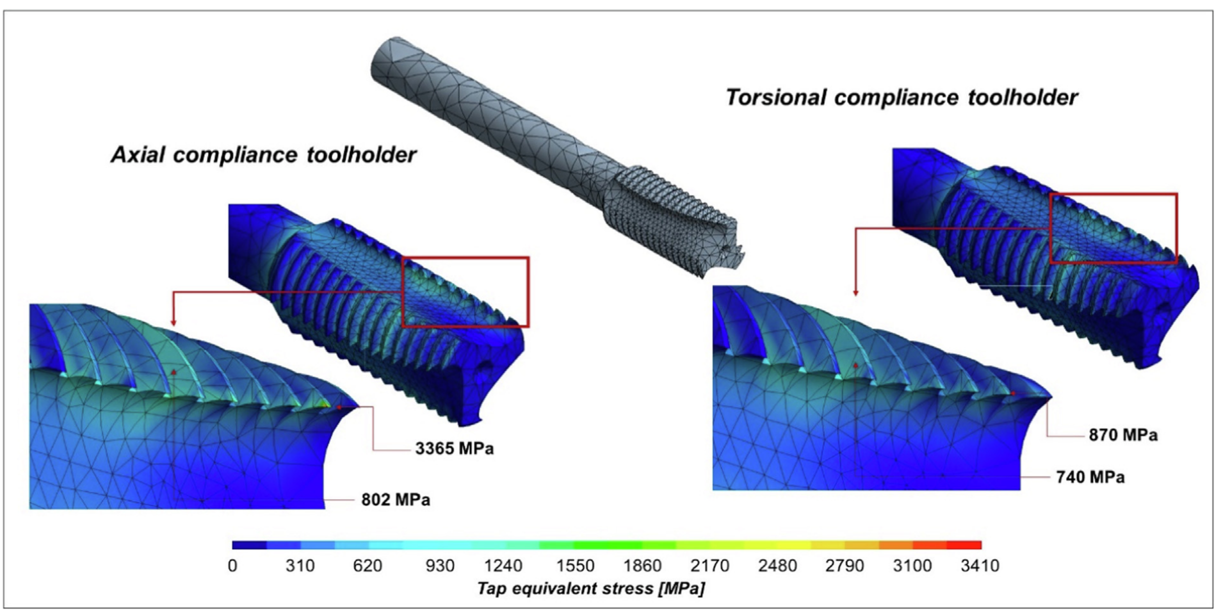

Fig. 8 Equivalent stress caused by cutting taps.

is the sixth tooth, where 802 MPa and 740 MPa are obtained with the torsional compliance toolholder and the proposed one, respectively. In this case, using the torsional compliance toolholder implies a reduction of ≈8% in the equivalent stress. On the other hand, when the maximum value and the next one are compared under the same situation, in the case of the axial compliance toolholder, the difference between them is ≈76 % and ≈15 % in the case of using the torsional compliance toolholder. Therefore, with the simulations, it is demonstrated that not only is the maximum stress using the proposed toolholder reduced but also its use implies greater stability in the cutting tap cutting edges, and thus a more robust and reliable process is obtained.

Once it was numerically demonstrated the suitability of the proposed toolholder, its efficiency was analyzed from an empirical point of view. Fig. 9 shows tool wear and power consumption results from the first test stage. Regarding the power consumption, the maximum one is registered just at the moment feed inversion and tapping tool rotation is reversed. The average one is related with the average values of the tapping process when the thread is machining. In the case of the maximum power consumption, the value graphed in each thread corresponds to the average of the values obtained in the three tests. In the same way, the average values graphed were obtained. In this case, in each test, the average value of each thread was obtained by taking the values registered when the tapping tool is threading. Once these values were obtained in the three tests, the values graphed were the mean of these

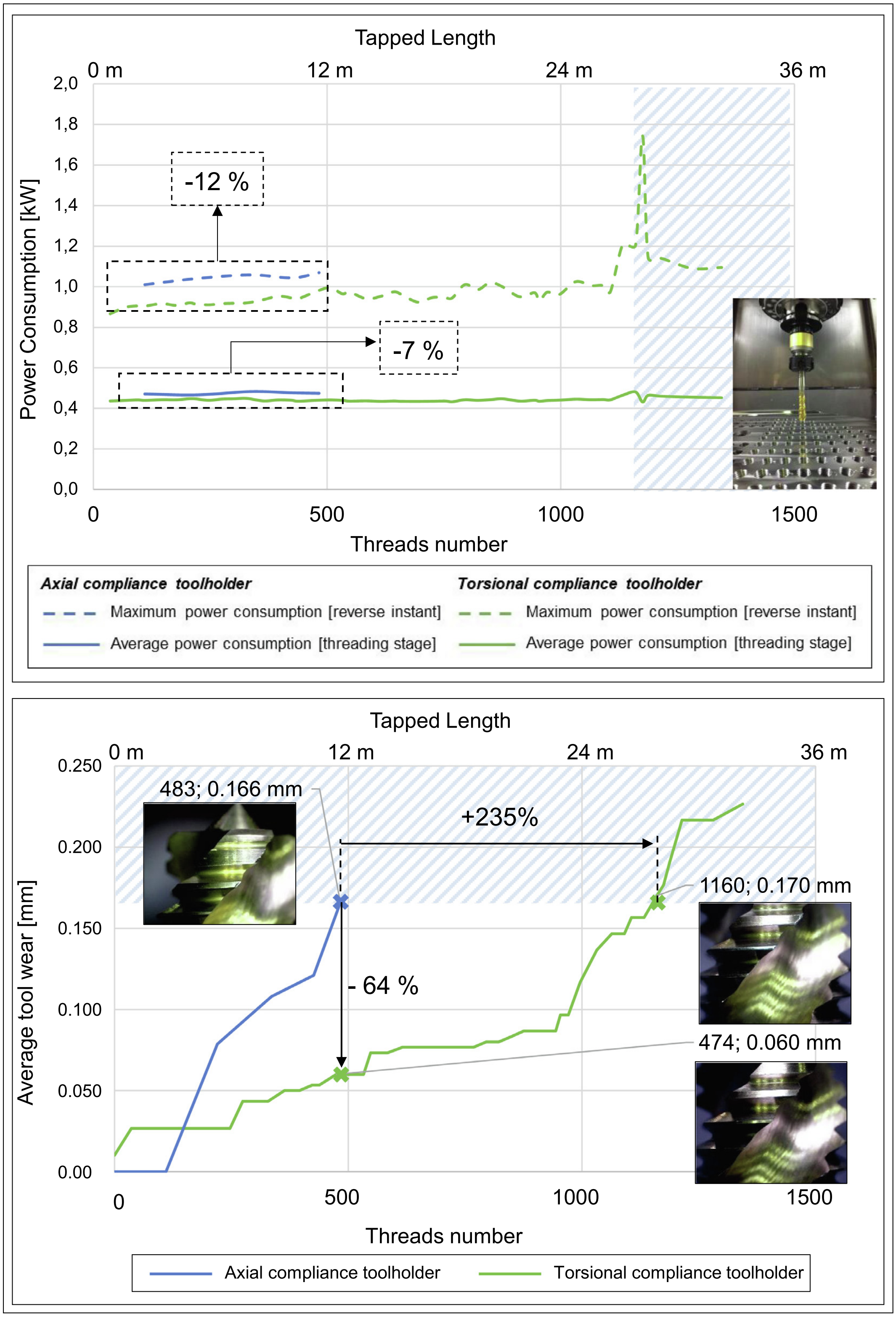

Fig. 9 Power consumption and tool wear results.

three values. Focusing on the average power consumption, in the case of using the new torsional compliance toolholder, the values obtained are reduced a 7 % in comparison with the axial compliance one. This behavior is even enhanced in the maximum power consumption. In this case, the difference between both toolholders is 12 %, with the values lower in the case of using the new one caused by the better synchronism in which the system absorbs the errors in the reversion movement instant. Consequently, the torsional compliance toolholder implies a smoother tapping process that avoids overstressing phenomenon on the tapping tool and, therefore, higher tool life as seen in the tool wear graph.

Regarding tool wear, it must be noted that using ISO 3685 minimum tool life criterion was not achieved in any case. In both cases, the "go/no go" gauge was the stop criterion that was achieved first when edge wear achieved ≈0.170 mm. In particular, when the axial compliance toolholder was used, 483 threads were carried out until ending the test with tool wear of 0.166 mm. Nevertheless, at this stage, the tool wear's torsional compliance was lower by 65 %, achieving the same tool wear at thread number 1,160 with tool wear of 0.170 mm, an increase of 235 % when this toolholder is used.

In addition, Fig. 10 shows the final stages of cutting taps edges when axial and torsional compliance toolholders were used, respectively. The results show that when the tool tap used with the axial compliance toolholder achieves the stop criterion, it presents notch wear and abrasive wear, respectively, provoking the irregularity of the main edge. However, at this stage, the tool tap used with the torsional compliance toolholder presented slight wear, reaching similar tool wear after machining 1,160 threads due to the improvement of the synchronism between rotational and vertical movements and, consequently, achieving a tapping process more secure and reliable.

Once the improvement using the new torsional compliance toolholder was demonstrated empirically, the optimization of cutting parameters was carried out through tests in which the conventional cutting speed (15 m/min) was taken as reference, and it was increased and decreased by 35 %, respectively; that is, 20 m/min and 10 m/min cutting speeds were tested. Fig. 11 and Fig. 12 show the results obtained regarding power consumption and tool wear, respectively.

The average power consumption was reasonably analogous for all cutting speeds tested, presenting small differences with no particular significance. In the case of maximum power consumption at the reverse stage, the values were similar, except for the 10 m/min test. In this case, the power consumption reduction was ≈30 %. Nevertheless, despite obtaining this reduction, the cutting tap was broken catastrophically in tap 1,038 due to the high torque presented by this cutting speed

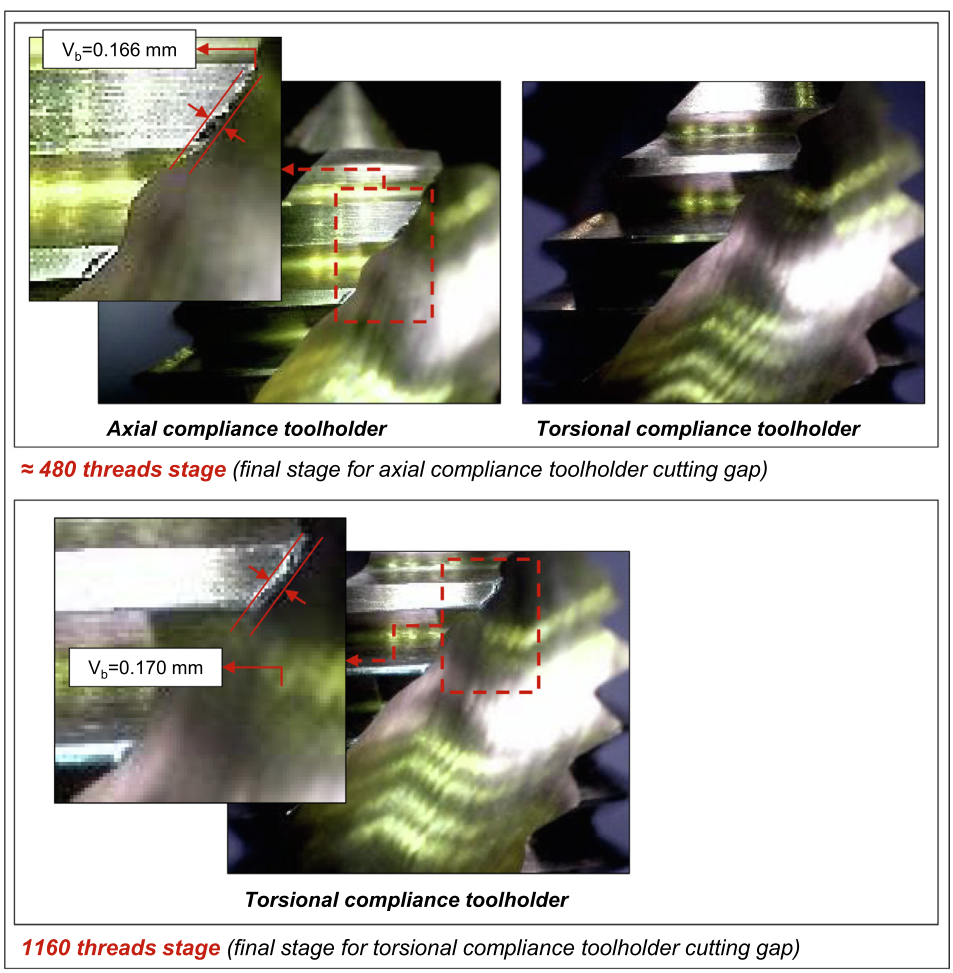

Fig. 10 Tool wear at final tool life stages.

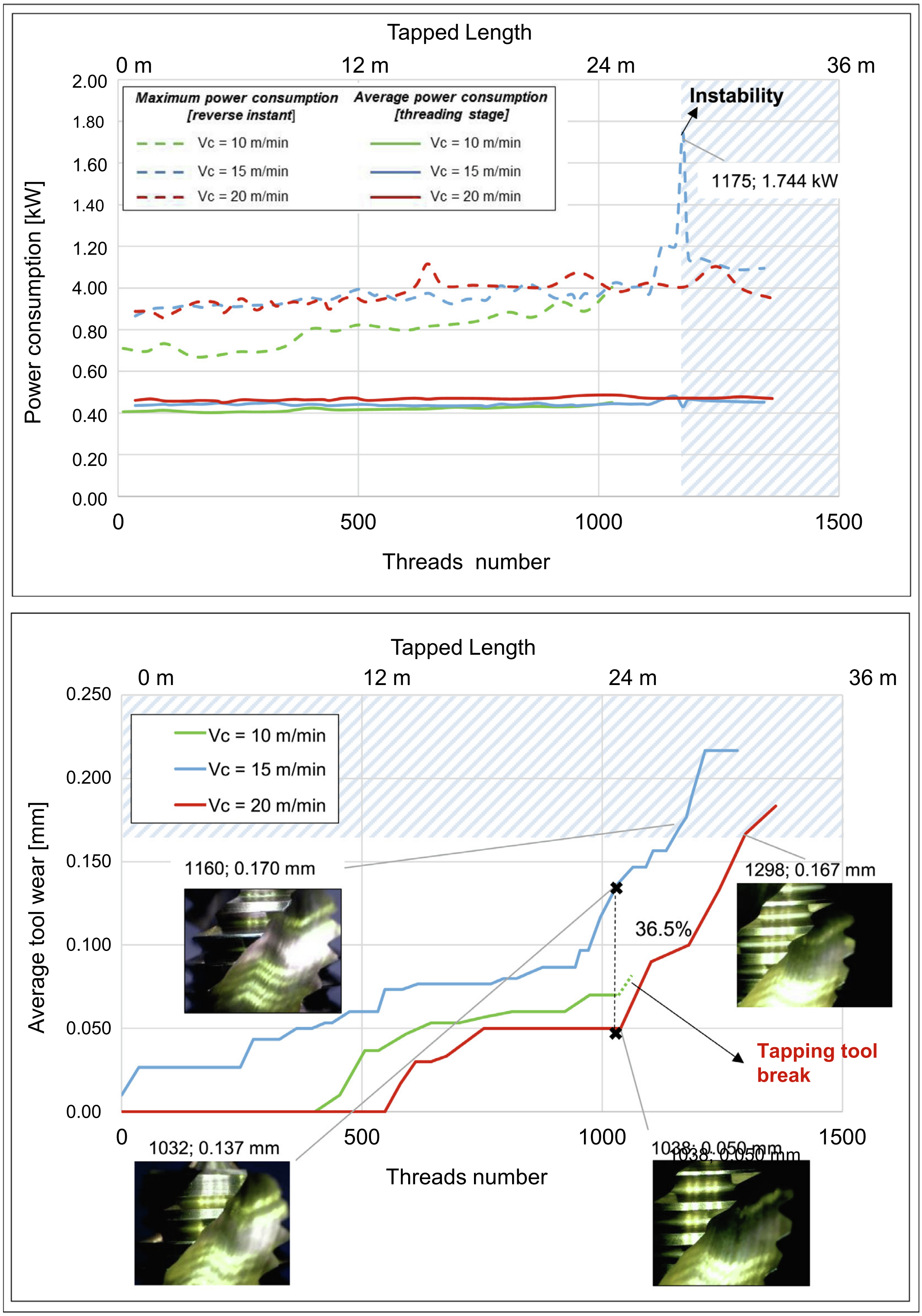

Fig. 11 Power consumption and tool wear obtained with torsional compliance toolholder.

compared with the reference (15 m/min); this implies a tool life reduction of ≈12 %. Therefore, this cutting speed is discarded for being used industrially.

On the other hand, when 20 m/min is used as cutting speed, a more reliable and robust process is achieved. Analyzing tool wear, the percentage of tool life at 1,038 – the nearest point to final tool life with 10 m/min cutting speed in which tool wear was measured – the difference with the reference (15 m/min) is 36.5 % less. Besides, the cutting tap, in this case, achieved 1,361 taps before ending the test due to the "go/no go" gauge criterion, improving tool life by ≈20 % in comparison with the reference cutting speed. Overall, tapping at the lowest veloci-

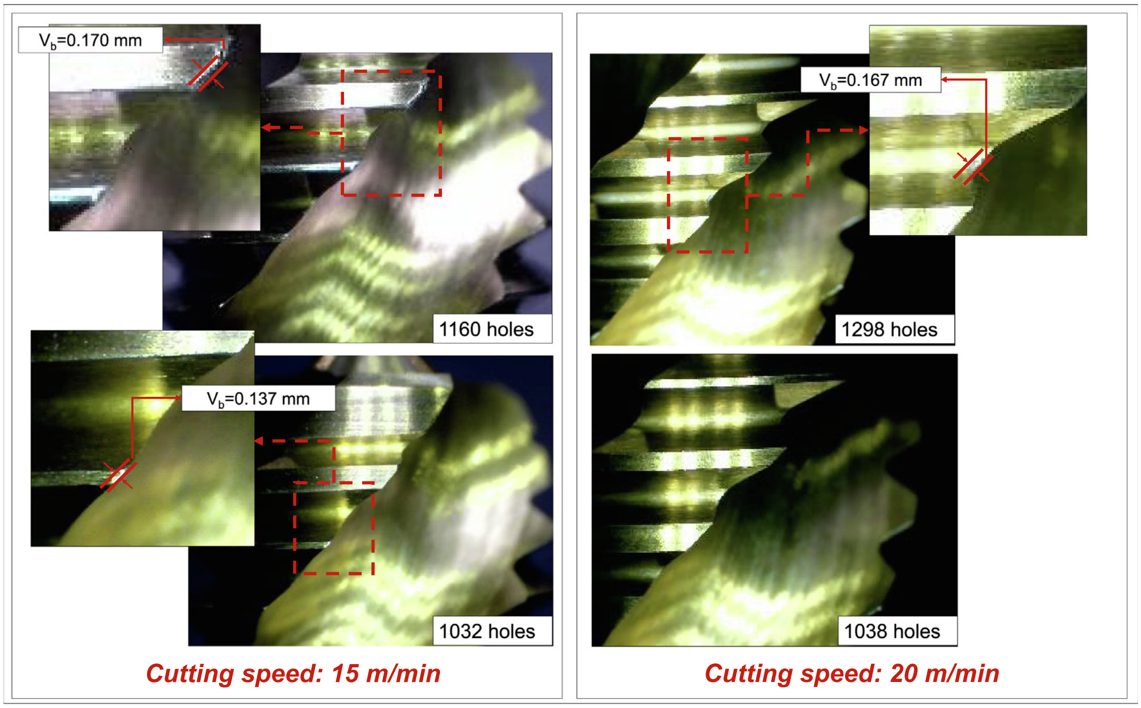

Fig. 12 Tool wear at different tool life stages.

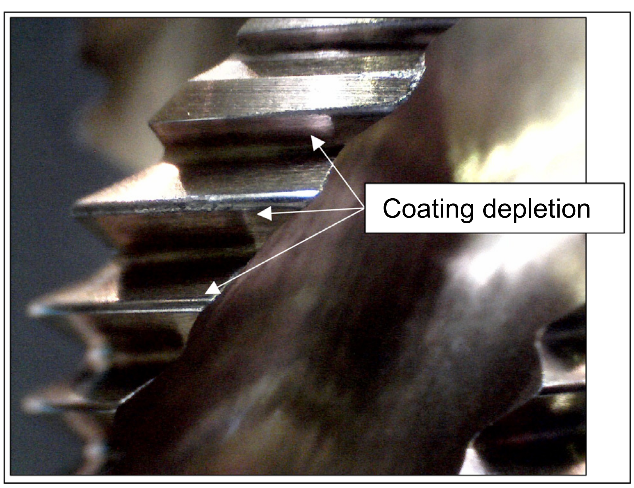

Fig. 13 Tool wear before catastrophic failure at 10 m/min.

ties (10 m/min) implies catastrophic failure and the thread sculpting at the highest speeds (20 m/min) provokes an increase in tool life with a similar spindle power consumption.

Concerning tool wear evolution, as mentioned above, cutting taps in the case of using 10 m/min as cutting speed were broken catastrophically after 1,038 threads. This premature failure was caused because with this cutting speed the tapping process is nearer of plastic deformation instead of an effective cutting process where the coating not only is suppressed along the edge due to the friction between the material and the tool but also in the incidence edge as can been seen in Fig. 13.

On the other hand, at 10 m/min tool failure stage, when 15 m/min is used the cutting tap presented 0,137 mm of flank wear and was practically negligible with 20 m/min. In these cases, at their final tool life stages (1,160 and 1,298 holes, respectively) presented similar tool wear mechanisms. In particular, notch and abrasion tool wear was observed, causing defective threads and therefore stopping the tests under the ""go/no go" gauge" criterion. This behavior is in line with the work carried out by Chede et al. 2022 where a cutting speed increase implied an increase of tool life until achieving a turning point [30]. In the present case, this tool life increase is caused by the improvement of tool holder, which allows to reach this cutting speed value because its use implies an improvement of the toolholders performance based on a higher stiffness due to the torsional compliance which improves the robustness of the process.

Regarding surface integrity, Fig. 14 shows histograms and their thread topographies obtained with an infinite-focus Alicona® microscope at different stages with the axial compliance toolholder at 15 m/min (conventional cutting speed) and torsional compliance toolholder at 20 m/min (improved cutting speed). In particular, the stages analyzed were when the tapping tool cutting edge achieved 0.05 mm, 0.1 mm and 0.17 mm, respectively, in order to observe any difference caused by the toolholders under the same wear performance in the thread surfaces.

Hence, regarding surface roughness values, the results show that in the case of using the torsional compliance toolholder, the improvement is evident, obtaining lower values in average surface roughness (R_a) and the mean values of five consecutive maximum heights between peak-valley (R_z). In particular, at the first stage, the difference between R_a was ≈35 % and 25 % for R_z, reducing this difference until it reached the final stage, in which the difference was ≈1.5 % and ≈1%, respectively. Results are quite similar, but in the case of the torsional compliance toolholder, with an increase of threads carried out of 20 %, as discussed above. Besides, in the case of analyzing

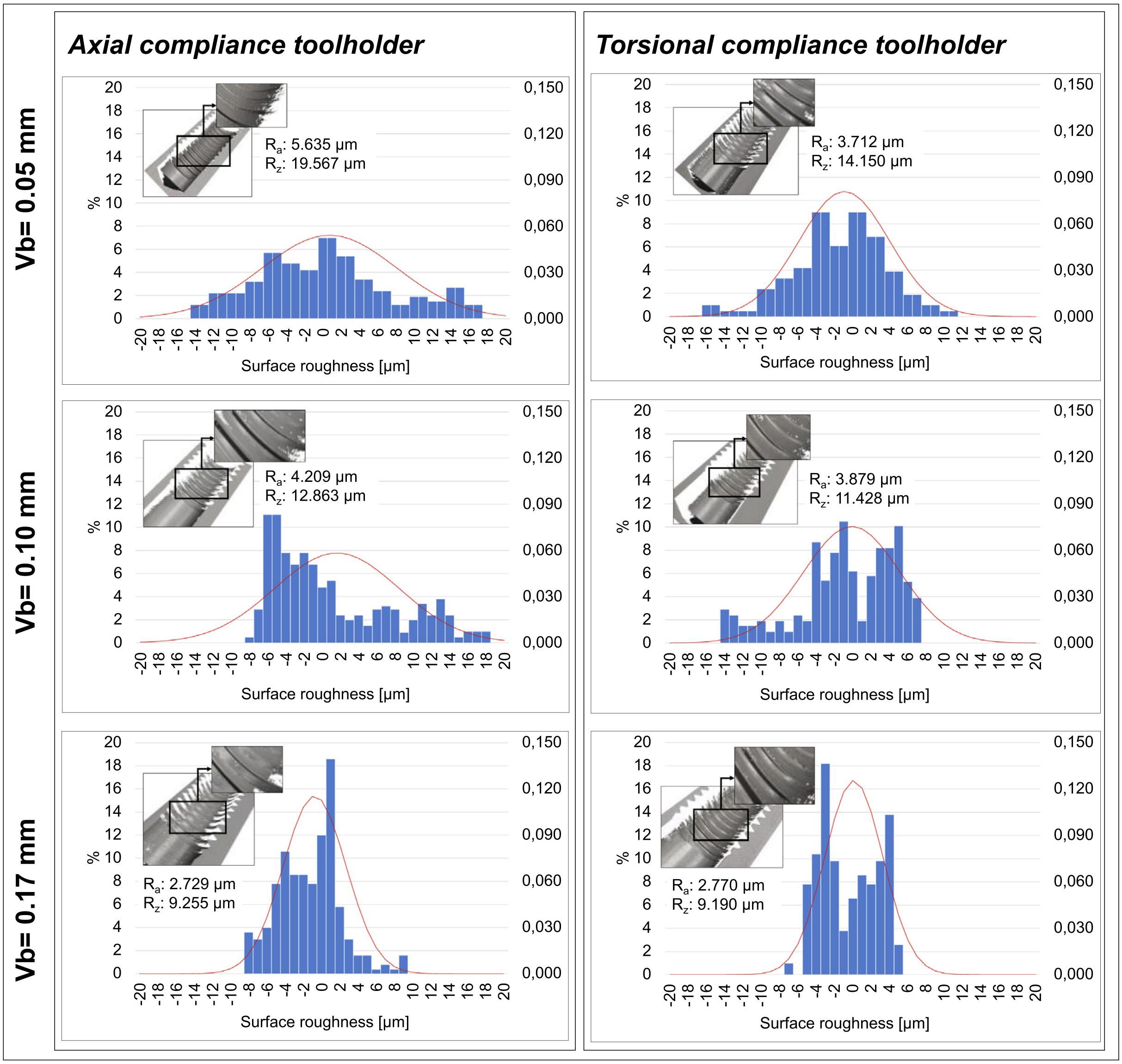

Fig. 14 Thread surfaces histograms and topographies at different stages with each toolholder.

the thread quality, the use of the new toolholder also implied reducing abrasion and notch phenomenon on the main edge and the clearance faces of the tap from the process in the thread profiles from the first stage until the last one, keeping in perfect conditions the main edge of tap and, consequently, achieving a more suitable process in which the stability of the process is guaranteed.

Therefore, the use of the new rotational compliance tool holder implies keeping a stable process in which thread surface integrity is improved; power consumption is stabilized due to the energy of synchronization errors absorbed when cutting tap changes the rotation direction; and consequently, an increase of productivity through the increase of tool life and cutting speed.

4. Conclusions

This work proposes a new torsional compliance toolholder for tapping operations. The new toolholder is characterized by being provided with elastic metal pins instead of having conventional springs. The viability of this toolholder was analyzed in comparison with a conventional axial compliance toolholder, in which power consumption, tool life and threads surface integrity were taken into account. The main conclusions obtained from the simulations and the battery of tests carried out are listed below:

- The use of the torsional compliance toolholder implies a 75 % reduction of the maximum equivalent stress in comparison with the axial compliance toolholder in the tapping reversion instant stage and implies greater stability in the tap cutting edges obtaining a difference between the maximum value and the next one of 15 % instead of 76 % achieved by the axial compliance toolholder.
- The use of a torsional compliance toolholder implied, in the case of using 15 m/min (conventional cutting speed), a reduction of power consumption compared with the axial compliance toolholder in the tapping reversion instant stage of 12 %. Besides, in this case, tool life is increased a 235 % until the "go/no go" gauge stop criterion is achieved.

- The new torsional compliance tool holder allows an increase of cutting speed of 35 % without affecting tool life compared to the axial compliance toolholder case. In fact, tool life is increased by 20 %.
- Adhesion wear on tap's main edges and the clearance faces is less when using the torsional compliance tool holder.
- The thread quality is better when a torsional compliance toolholder is used. In particular, lower surface roughness is obtained along the tapping tool life and less adhesion on the thread profiles is observed.
- In all the tests, using a torsional compliance toolholder implied keeping a stable power consumption level. Consequently, the cutting forces are also controlled mainly due to the energy of synchronism errors in the tool rotation change stage being absorbed by the toolholder, guaranteeing the process stability.
- Vibration and how to expand the ideas to vibrational problems [28] from tapping [29] are the next step in research.

For all of the above reasons explained above, from a stability and productivity point of view, the use of the proposed torsional compliance toolholder implies not only an increase in tool life but also an increase in cutting speed and, accordingly, a time reduction of the manufacturing processes, in which also threads surface integrity is improved, achieving a real improvement in threads manufacturing.

Declaration of Competing Interest

The authors declare that they have no known competing financial interests or personal relationships that could have appeared to influence the work reported in this paper.

Acknowledgments

Authors owe deep thanks to Basque Government university group IT 1573, High performance machining, MiCINN PDC2021-121792-I00 New cutting tools production for manufacturing high added-value turbomachinery components with the acronym: HCTAYLOR and UPV/EHU for the predoctoral grant PIF 19/96. Also, the authors thank Grant PID2019-109340RB-I00 funded by MCIN/AEI/10.13039/501100011033. Finally, the authors would like to make special mention of LAIP's involvement in the development of the tool holder under the HAZITEK program from the Department of Economic Development and Infrastructures of the Basque Government and FEDER funds, related to the project with the acronym CORTEX.

References

[1] S. Bhowmick, M.J. Lukitsch, A.T. Alpas, Tapping of Al-Si alloys with diamond-like carbon coated tools and minimum quantity lubrication, J. Mater. Process. Technol 10 (2010) 2142–2153.

[2] P. Monka, K. Monkova, V. Modrak, S. Hric, P. Pastucha, Study of a tap failure at the internal threads machining, Eng. Fail. Anal 100 (2019) 25–30.

[3] M.N. Armarego, P. Chen, Predictive models for the forces and torque in machine tapping with straight flute taps, Annals of CIRP 51 (2002) 75–78.

[4] J.S. Agapiou, Evaluation of the effect of high speed machining on tapping, J. Manuf. Sci. Eng. Trans. ASME 116 (1994) 457–462.

[5] J.H. Ahn, D.J. Lee, S.H. Kim, H.Y. Kim, K.K. Cho, Effects of synchronizing errors on cutting performance in the ultra-high-speed tapping, CIRP Ann. - Manuf. Technol 52 (2003) 53–56.

[6] K. Gawdzinska, Application of the Pareto chart and Ishikawa diagram for the identification of major defects in metal composite castings, Archives Foundry Eng. 11 (2019) 290–299.

[7] G. Uzun, İ. Korkut, The effect of cryogenic treatment on tapping, Int J Adv Manuf Technol 67 (2013) 857–864.

[8] A. Gil Del Val, P.M. Diéguez, M. Arizmend, M. Estrems, Experimental study of tapping wear mechanisms on nodular cast iron, Procedia Eng. 132 (2015) 190–196.

[9] I.C. Pereira, M.B. Da Silva, D.F. Da Cunha, W. Falco, Analysis of tapping process in three types of cast iron, Int J Adv Manuf Technol 82 (2016) 1041–1048.

[10] I.C. Pereira, M.B. Da Silva, Study of the internal thread process with cut and form taps according to secondary characteristics of the process, Int. J. Adv. Manuf. Technol 93 (2017) 2357–2368.

[11] A. Oliveira, G. Vilela, M. Bacci, E. Silva, Rosqueamento interno usando macho de corte com utilização da mesa compensadora e do cabeçote flutuante, 27° Posmec 11-13 September 2017.

[12] I. Elosegui, U. Alonso, L.N. López de Lacalle, PVD coatings for thread tapping of austempered ductile iron, Int. J. Adv. Manuf. Technol 91 (2017) 2663–2672.

[13] A. Zawada-Tomkiewicz, I. Wierucka, A case study in technological quality assurance of metric screw thread, Measurement 114 (2018) 208–2017.

[14] S.A. De Freitas, J.T. Vieira, S.L.M.R. Filho, L. Cardoso, Experimental investigation of tapping in CFRP with analysis of torque-tension resistance, Int. J. Adv. Manuf. Technol 104 (2019) 757–766.

[15] J. Ni, G. Feng, Z. Meng, T. Hong, Y. Chen, X. Zheng, Reinforced lubrication of vegetable oils with graphene additive in tapping ADC12 aluminum alloy, Int J Adv Manuf Technol 94 (2018) 1031–1040.

[16] G. Lorentz, Principal component analysis in technology, Annals of CIRP 38 (1989) 107–109.

[17] Y.B. Chen, J.L. Sha, S.M. Wu, Diagnosis of tapping process by information measure and probability voting approach, J. Eng. Ind. 112 (1990) 319–325.

[18] T. Liu, E.J. Ko, S.L. Sha, Diagnosis of tapping processes using an AI approach, J Mater Shaping Tech 9 (1991) 39–46.

[19] W. Li, D. Li, J. Ni, Diagnosis of tapping process using spindle motor current, Int. J. Mach. Tool Manuf. 43 (2002) 73–79.

[20] O.A. Mezentsev, R.E. DeVor, S.G. Kapoor, Prediction of Thread Quality by Detection and Estimation of Tapping Faults, J. Manuf. Sci. Eng 124 (2002) 643–650.

[21] A. Gil Del Val, J. Fernández, E. Del Castillo, M. Arizmendi, F. Veiga, Monitoring of thread quality when tapping nodular cast iron with TiN-coated HSS cutting taps, Int. J. Adv. Manuf. Technol 69 (2013) 1273–1282.

[22] I.C. Pereira, P.I. Vianello, D. Boing, G. Guimarães, M. Bacci da Silva, An approach to torque and temperature thread by thread on tapping. Int J Adv Manuf Technol 106 (2020) 4891–4901.

[23] R. Polvorosa, L.N. López de Lacalle, A.J. Sánchez, A. Fernández, M. Esparta, I. Zamakona, Cutting edge control by monitoring the tapping torque of new and resharpened tapping tools in Inconel 718, Int J Adv Manuf Technol 106 (2020) 3799–3808.

[24] A. Gil Del Val, F. Veiga, O. Pereira, L.N. López De Lacalle, Threading performance of different coatings for high speed steel tapping, Coatings 10 (2020) 10–464.

[25] B. Dos Santos Siqueira, S.A. Freitas, R.B.D. Pereira, C.H. Lauro, L. Cardoso, Influence of chip breaker and helix angle on cutting efforts in the internal threading process, Int J Adv Manuf Technol 102 (2019) 1537–1546.

[26] M. Wan, Y.C. Ma, J. Feng, W.H.G. Zhang, Mechanics of tapping process with emphasis on measurement of feed error and estimation of its induced indentation forces, Int. J. Mach. Tools Manuf 114 (2017) 8–20.
[27] G. Urbikain, D. Olvera-Trejo, M. Luo, K. Tang, L.N. López de Lacalle, A. Elías-Zúñiga, A model-based sustainable productivity concept for the best decision-making in rough milling operations, Measurement 186 (2021).
[28] G. Urbikain, L.N. López de Lacalle, F.J. Campa, A. Fernández, A. Elías, Stability prediction in straight turning of a flexible workpiece by collocation method, Int. J. Mach. Tools Manuf 54 (2012) 73–81.
[29] J. Fernández Landeta, A. Fernández-Valdivielso, L.N. López de Lacalle, Wear of form taps in threading of steel cold forged parts, Journal of Manufacturing Science and Engineering 137 (2015) 031002.
[30] S.J. Chede, M.K. Chopra, N.B. Dhokey, V.S. Aher, P. Ghosh, Performance analysis of cryoprocessed conventional HSS M2 drill and P/M HSS M3 TiN coated tap and its effect on the substructure, Mater. Today: Proc. 65 (2022) 396–400.